MULTIPLE UAV FORMATION RECONFIGURATION WITH COLLISION AVOIDANCE GUIDANCE VIA DIFFERENTIAL GEOMETRY CONCEPT

Joongbo Seo* , Youdan Kim* , A. Tsourdos , B. A. White****
*** Seoul National University, Seoul 151-744. Republic of Korea.,**
****Cranfield University, Shrivenham, Swindon, Wiltshire SN6 8LA, United Kingdom.**
sjb@snu.ac.kr; ydkim@snu.ac.kr; a.tsourdos@cranfield.ac.uk; b.a.white@cranfield.ac.uk

Keywords: *UAV, Formation, Reconfiguration, Collision, Avoidance*

Abstract

In this paper, guidance law based on differential geometry is proposed for UAV formation flight and collision avoidance. The proposed guidance strategy makes it possible for multiple UAVs to avoid obstacle and maintain formation simultaneously. The decision making protocol determines whether formation fleet preserves their geometrical format during the manoeuvre of obstacle avoidance or not. Differential geometry uses the line of sight angle and relative velocity vector information, and therefore it may generate the excessive control input, which should be carefully treated. To maintain the formation, formation reconfiguration strategy is developed to make guidance command split the current formation up into sub group and therefore guidance control is distributed to each group for collision avoidance. Lyapunov candidate function is used to guarantee the stability of the proposed guidance strategy. Numerical simulation is performed to verify the performance of the proposed formation reconfiguration and guidance strategy.

1 INTRODUCTION

Advances in technology have made it possible to utilize autonomous unmanned aerial vehicles(UAVs) in teams to accomplish various missions. Especially, the small UAVs are capable of performing a variety of tasks ranging from reconnaissance to strategic attack. The use of fleets of UAV instead of a single aerial vehicle offers improved strategic return through longer baseline observations, enables faster ground track repeats, and provides a high degree of redundancy and reconfigurability in the event of a single vehicle failure. These benefits can be achieved at the expense of more stringent requirements on fleet coordination.

Since it is not easy to develop the algorithm which satisfies formation keeping and collision avoidance performance at the same time, lots of research are performed separately. Especially, numerous research studies have been done for conflict detection and resolution. [1], [2] investigated the application of differential geometry to UAV Conflict Detection and Resolution(CDR) algorithm for non-cooperating intruders. Whilst there exists region which the UAV cannot resolve due to its physical and operational limitations as every CDR algorithms have, the resolution guidance can find the region and prove local stability using Lyapunov theory. Besides, [3] used well-known proportional navigation guidance law to guide the follower UAV to the desired position using a velocity command. Also, researchers proposed the minimum maneuver radius for the leader UAV to prevent deformation by the excessive maneuver of the leader. In [4] and [5], a collision cone approach is used to predict any possible collision with the obstacle. If necessary, an alternate aiming direction is computed for reactive obstacle avoidance of UAVs. They extended algorithms for collision avoidance with both non-cooperative as well as cooperative environments. In [6], the authors considered a heterogeneous multi-UAV system using the nonlinear 6-DOF rigid body dynamics involved in close formation flight which has versatility to handle any formation geometry (V-type, echelon type, etc.)

In this paper, for the formation flying to the goal point, differential geometry guidance is adopted to avoid collision with non-manoeuvring obstacle. The proposed guidance strategies attempt to quickly align the velocity vector of the vehicle along the aiming point, which ensures quick reaction for the safety of the vehicle. When it comes to inevitable collision, formation is divided into subgroup and reconfigured. Escaping from the crisis of collision, reconfigured subgroup keeps tracking the goal point. Decision making procedure, which judges whether or not (i) fleet is under the risk and (ii) formation pattern is preserved, plays a key role in this process. In this study, five manoeuvering UAVs and non-manoeuvring obstacle is considered in the numerical simulation.

The rest of this paper is addressed as follows. First, section 2 deals with problem formulation including definition and assumption. Section 3 provides the decision making process with acceleration limit. Section 4 discusses the formation reconfiguration process, and section 5 describes the stability issue of the proposed guidance algorithm. Section 6 shows the simulation results. Concluding remarks are given in section 7.

2 PROBLEM FORMULATION

2.1 Definition and Assumption

Several definitions and assumptions are proposed, which will be used in this study.
First, it is assumed that collision occurs when the distance between the vehicle is shorter than safety radius R_p. Note that the collision between UAV and obstacle is only considered in this study. It is also assumed that each vehicle in formation has enough safety range initially, and common guidance command is distributed to each vehicle to preserve formation pattern.
Second, V-shape formation pattern is adapted which is complex of echelon formation and agents are arranged diagonally. Tactically, echelon formation is used to provide each vehicle in the formation an excellent range of vision. In particular, it is commonly employed by combat aircraft, where the close, streamlined flight formation can allow the planes to reduce fuel consumption by “surfing" the updraft created by the wingtip vortices of the aircraft ahead.

Let us consider point mass in 3-dimension to verify the proposed formation reconfiguration guidance.

$$\begin{aligned} \dot{x} &= V\cos\gamma\cos\psi \\ \dot{y} &= V\cos\gamma\sin\psi \\ \dot{z} &= V\sin\gamma \\ \dot{V} &= 0 \\ \dot{\gamma} &= (\gamma_c-\gamma)/\tau_\gamma \\ \dot{\psi} &= (\psi_c-\psi)/\tau_\psi \end{aligned} \tag{1}$$

where the state vector $X=[x,y,z,V,\gamma,\psi]^T$ denotes the inertial position (x,y,z) of the UAV, the ground speed, heading angle, and flight path angle, respectively. The control input vector $U=[\gamma,\psi]^T$ denotes heading angle, and flight path angle command, respectively. Let us assume that the ground speed of UAV is constant during the flight, and UAV obtains the position and velocity vector information using communication equipment and sensors.

2.2 General Concept of Collision Avoidance with Formation Keeping

Let us consider the case that all of the agents avoid obstacle preserving formation format. In order to keep the formation, differential geometry (DG) control command from leader UAV may be applied to every vehicle at the same time. However, it can cause collision between followers and obstacle. Figure 1 shows the concept of differential geometry for the collision avoidance. In Fig.

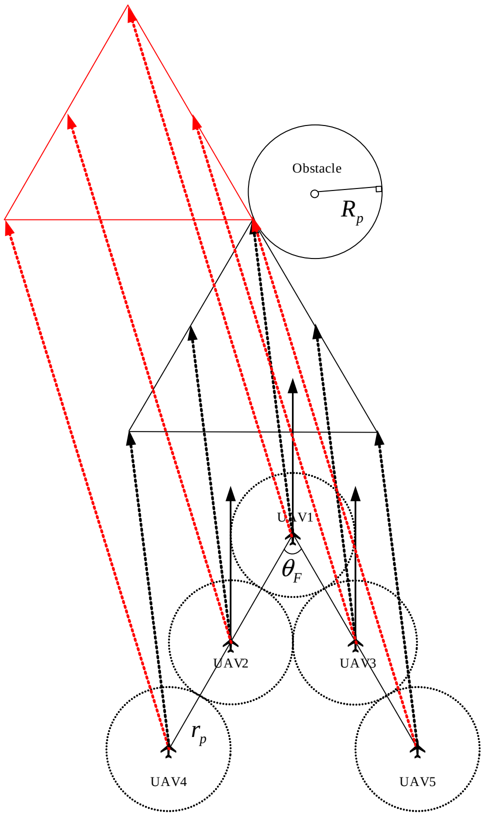

Fig. 1 Collision Avoidance via Differential Geometry

1, the solid black lines present velocity vectors of each vehicle. The dotted black lines show the trial desired velocity vectors, and the dotted red lines are the final desired velocity vectors.

Using DG control command for each follower UAV can cope with the collision as follows.

1. With the DG command of leader vehicle, decision of the direction can avoid collision.

2. There are two possible cases.
   Case 1) If the leader selects left turn, DG control command of the rightmost follower is applied to every vehicle.
   Case 2) If the leader selects right turn, DG control command of the leftmost follower is applied to every vehicle.

This type of control scheme is reasonable when the formation shape is triangle type. If the desired vector, which is the outermost from the selected formation pattern is a priorily known, then it is possible to manage the decision making appropriately.

All of the agents cannot avoid obstacle while preserving formation format, since the velocities cannot exceed the minimum and maximum velocity or reduce below the minimum velocity. Also, the limitation of maximum angular rate can influence on the collision avoidance manoeuvre.

2.3 Completeness of Collision Avoidance Guidance

In the previous research on DG based guidance, collision cone approach is used to predict any possible collision with the obstacle. And, if necessary, an alternate aiming direction is computed for reactive obstacle avoidance of UAVs.[4]-[5]

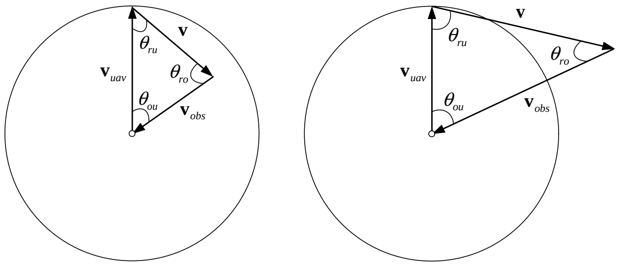

Fig. 2 Velocity relationship geometry

As shown in Fig. 2, the angle information between velocity vector of UAV and velocity vector of obstacle can be obtained. In Fig. 2, a circle is defined by UAV velocity vector. The velocity and relative velocity of UAVs can be expressed as follows

$$\begin{aligned} \mathbf{v}_{uav} &= \mathbf{v} + \mathbf{v}_{obs} \\ v_{uav}\mathbf{t}_{uav} &= v\mathbf{t} + v_{obs}\mathbf{t}_{obs} \\ \mathbf{t}_{uav} &= \alpha\mathbf{t} + \beta\mathbf{t}_{obs} \end{aligned} \tag{2}$$

where $\mathbf{t_{uav}}$ and $\mathbf{t_{obs}}$ denote the unit vector tangent to UAV and obstacle velocity vector, respectively, v_{uav} and v_{obs} denote the magnitude of the corresponding vectors, and

$$\alpha = \frac{v}{v_{uav}}, \quad \beta = \frac{v_{obs}}{v_{uav}} \tag{3}$$

From Fig. 2, the relative velocity angles are given by

$$\begin{aligned}\theta_{ou} &= \theta_u - \theta_o\\ \theta_{ru} &= \theta_u - \theta_r\\ \theta_{ro} &= \theta_o - \theta_r\end{aligned} \tag{4}$$

where θ_u and θ_o are the heading angles of the UAV and obstacle, and θ_r is the relative velocity angle. The sine and cosine rules on the velocity vectors give

$$\begin{aligned}\sin\theta_{ru} &= \beta\sin\theta_{ro}\\ \cos\theta_{ru} &= \pm\sqrt{1-\beta^2\sin{\theta_{ru}}^2}\end{aligned} \tag{5}$$

Using sine rule, we have

$$\begin{aligned}v_u^2 &= v^2 + v_o^2 - 2vv_o\cos\theta_{ro}\\ v &= v_o\cos\theta_{ro} \pm\sqrt{v_u^2 - v_o^2\sin\theta_{ro}}\end{aligned} \tag{6}$$

Therefore, the magnitude of the desired relative velocity vector $\widehat{v}$ can be represented as

$$\begin{aligned}\hat{v} &= v_o\cos\hat{\theta}_{ro} \pm\sqrt{\lambda(\hat{\theta}_{ro})}\\ \lambda(\hat{\theta}_{ro}) &= v_u^2 - v_u^2\sin^2\theta_{ro}\end{aligned} \tag{7}$$

where $\hat{\theta}_{ro} = \theta_o - \hat{\theta}_r$. Note from Eq. (7) that is possible to derive the desired relative velocity vector, which is tangent to the sector of obstacle, when the speed of obstacle is not faster than that of UAV.

3 DECISION MAKING PROCESS IF ACCELERATION IS OVER THE LIMIT

Let us consider V_{min} and V_{max} which are constant limitation on UAV velocity, according to stall speed and physical engine limit of aircraft. The acceleration a_{cent}, a centripetal force at outermost vehicle, can be expressed as

$$a_{cent} = \frac{V_{FLN}^2}{R_{FLN}} \tag{8}$$

where V_{FLN} is the velocity of leader UAV, and R_{FLN} is the longest radius of the outermost UAV. The aircraft F_{LN} means the n-th level vehicle in left branch. The constraint condition for the outermost vehicle can be related to the velocity and the radius of the leader. That is, the acceleration of the outermost vehicle should have the following limit.

$$a_{cent} = \frac{V_{FLN}^2}{R_{FLN}} \le f(V_L, R_L, V_{max}) \tag{9}$$

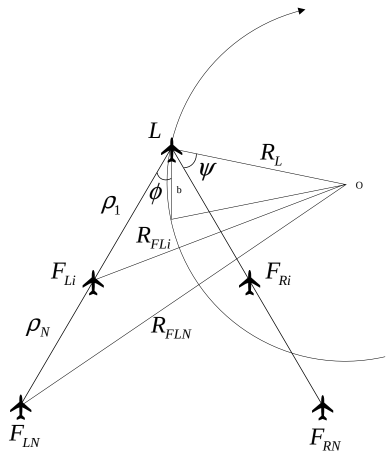

Fig. 3 Circular path for rotation manoeuvre

Now, let us consider the circular path as shown in Fig. 3. Using the trigonometry rule with OLF_{LN}, the longest radius R_{FLN} can be calculated as follows.

$$R_{FLN}^2 = R_L^2 + \rho_T^2 - 2R_L\rho_T\cos(B+2\psi) \tag{10}$$

where $\psi \doteq \frac{\pi}{2} - \phi$ when $b \gg R_L$, and $\rho_T = \rho_1 + \rho_N$. In order to maintain the formation pattern, all the angular velocity of each vehicle should satisfy the following relation.

$$\frac{V_L}{R_L} = \frac{V_{FLi}}{R_{FLi}} = \frac{V_{FLN}}{R_{FLN}} \tag{11}$$

where V_{FLi} and R_{FLi} are the velocity and radius of i-th follower, respectively.

From Eq. (11), we have

$$V_{FLN} = \frac{R_{FLN}}{R_L}V_L \le V_{max} \tag{12}$$

Squaring of both sides gives

$$\frac{R_{FLN}^2}{R_L^2}V_L^2 \le V_{max}^2 \tag{13}$$

Converting the left term into acceleration term, we have

$$\frac{R_{FLN}}{R_N^2}V_L^2 \le \frac{V_{max}^2}{R_{FLN}}$$
$$\frac{R_{FLN}}{R_L^2}V_L^2 \le \frac{V_{max}^2}{\sqrt{R_L^2+\rho_T^2-2R_L\rho_T\cos(\psi+2\phi)}} \tag{14}$$

Therefore, the following condition is obtained.

$$a_{FLN} \le \frac{V_{max}^2}{\sqrt{R_L^2+\rho_T^2-2R_L\rho_T\cos(\psi+2\phi)}} = a_{Limit} \tag{15}$$

Rotation radius can be given with a current velocity and acceleration command as

$$R_L = \frac{V_L^2}{a_{cmd}} \tag{16}$$

If the generated acceleration command for the outermost vehicle exceeds the limit value of Eq. (15), the given formation should be dissolved to avoid the collision. In the subsequent section, a formation reconfiguration process will be discussed.

4 FORMATION RECONFIGURATION PROCESS AND GUIDANCE TRANSITION

4.1 Formation Reconfiguration Process

DG control command for a proper vehicle can deal with the collision avoidance and formation keeping issues at the same time. Figure 4 shows the formation reconfiguration process when the acceleration command is over the limit.

1. When collision avoidance manoeuvre for a leader decides right turn, all vehicles should use the same DG command for UAV 4 in Fig. 4.
2. If DG acceleration command for UAV 4 exceeds the limit, ($a_{FLN} > a_{Limit}$),
   (a) UAV 1, UAV 3, and UAV 5 switch the input acceleration command to DG command for the leader.
   (b) UAV 2 and UAV 4 are separated from the formation and perform the obstacle avoidance manoeuvre as a new sub group. New input DG command for the outermost vehicle, UAV 2, is applied to UAV 2 and UAV 4.

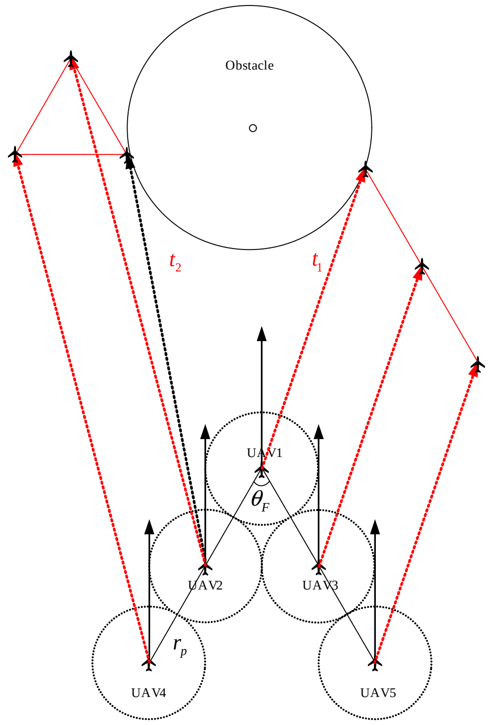

Fig. 4 Disjoint of 6 UAVs Formation fleet

4.2 Guidance Transition

The information of obstacles, for recognizing the obstacles as the object for collision avoidance, can be acquired by the following radar signal ζ.

$$\zeta = \begin{cases} 1 & if\ R_{ou} \le R_{rcg} \\ 0 & if\ R_{ou} > R_{rcg} \end{cases} \tag{17}$$

where R_{ou} is relative distance between the obstacle and UAV and R_{rcg}. Note that R_{rcg} is predefined recognition range. After detecting the obstacles, the final guidance command for *i-th* UAV is generated as follows.

$$u_i = \begin{cases} u_{G1} & if\ \zeta = 1 \\ u_{G2} & if\ \zeta = 0 \end{cases} \tag{18}$$

where, u_{G1} is a guidance command for the collision avoidance via DG, and u_{G2} is a guidance command for tracking the goal point. Note that u_{G1} is the input for the collision avoidance, u_{G2} is the goal point tracking guidance command, which are generated by classic guidance controller using position and flight path angle information.

• 3-dimensional expansion
Until now, guidance law based on DG in 2 dimensional XY plane is explained. Due to symmetry, the guidance problem in XY plane with control input ψ and the one in YZ plane with control input γ can be easily handled in same manner.

5 STABILITY ANALYSIS WITH DG

Figure 5 shows the schematic diagram for avoiding the obstacle using DG. The turning direction r_2 of UAV 2 can be decided by comparing ϕ and γ. Now, let us analyze the stability of the guidance law via differential geometry. Let us consider the following Lyapunov candidate function.

$$V = \frac{1}{2}\theta_e^2 \tag{19}$$

where $\theta_e = \hat{\theta}_r - \theta_r$, and θ_r and $\hat{\theta}_r$ are the current relative velocity and desired relative velocity angles of UAV, respectively. The stable guidance command should satisfy the following condition.[1]

$$\dot{\theta}_e \theta_e \leq 0 \tag{20}$$

From Eq. (5), we have

$$\begin{aligned} \theta_{ru} &= \sin^{-1}(\beta \sin\theta_{ro}) \\ \dot{\theta}_{ru} &= \pm\frac{\beta\cos\theta_{ro}}{\sqrt{1-\beta^2\sin^2\theta_{ro}}}\dot{\theta}_{ro} \end{aligned} \tag{21}$$

or,

$$\kappa(\theta_{ro}) = \pm\kappa(\theta_{ro})\dot{\theta}_{ro} \tag{22}$$

where $\kappa(\theta_{ro}) = \pm\frac{\beta\cos\theta_{ro}}{\sqrt{1-\beta^2\sin^2\theta_{ro}}}$ satisfies the following relation.

$$-\beta \leq \kappa(\theta_{ro}) \leq \beta \tag{23}$$

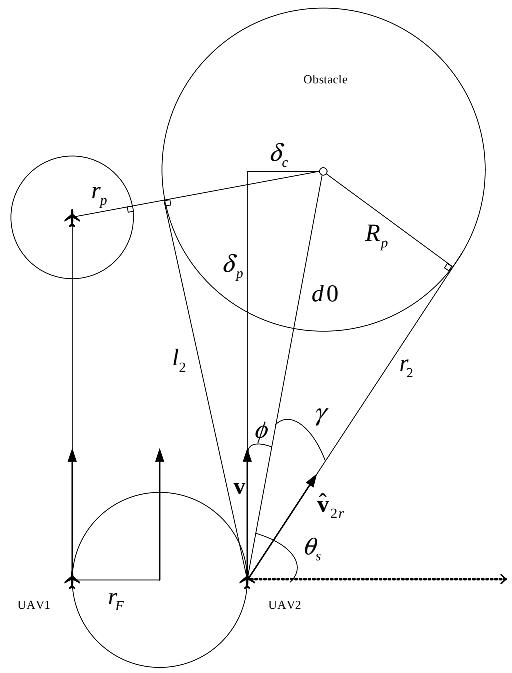

Fig. 5 How to avoid obstacle with DG

If UAV velocity v_u is larger than the obstacle velocity v_o, then the sign of $\kappa(\theta_{ro})$ depends on the angle θ_{ro} as

$$\kappa(\theta_{ro}) = \frac{\beta\cos\theta_{ro}}{\sqrt{1-\beta^2\sin^2\theta_{ro}}} sign\{\cos\theta_{ro}\} \tag{24}$$

From the above equations, the following equation can be obtained

$$\begin{aligned} \theta_{ou} &= 180 - \theta_{ru} - \theta_{ro} \\ \dot{\theta_{ou}} &= \dot{\theta_{ru}} - \dot{\theta_{ro}} \\ \dot{\theta_{ou}} + \dot{\theta_{ro}} &= \dot{\theta_{ru}} \\ \dot{\theta}_u - \dot{\theta}_r &= -\kappa(\theta_{ro})\dot{\theta}_{ro} \\ &= -\kappa(\theta_{ro})(\dot{\theta}_o - \dot{\theta}_r) \\ \dot{\theta}_u &= (1+\kappa(\theta_{ro}))\dot{\theta}_r - \kappa(\theta_{ro})\dot{\theta}_r \end{aligned} \tag{25}$$

In this study, it is assumed that the obstacle is not moving, and therefore we have

$$\dot{\theta}_u = (1+\kappa(\theta_{ro}))\dot{\theta}_r \tag{26}$$

Since $\dot{\theta}_u \leq \max[(1+\kappa(\theta_{ro})\dot{\theta}_r]$, the following relation is obtained.

$$\dot{\hat{\theta}}_u \leq (1+\beta)\max[\dot{\hat{\theta}}_r] \tag{27}$$

From Ref. [1], the following relation can be derived.

$$\max[\dot{\hat{\theta}}_r] \leq \frac{v}{\sqrt{d_0^2 - R_p^2}} \tag{28}$$

From Eq. (20) and Eq. (28), a heading angle rate can be represented as

$$\dot{\theta}_u = \frac{(1+\beta)v}{\sqrt{d_0^2 - R_p^2}} sign(\theta_e) + K\theta_e \tag{29}$$

where $K > 0$, and $sign(\theta_e) = \frac{|\theta_e|}{\theta_e}$. Finally, we have

$$\begin{aligned} \dot{V} &= \dot{\theta}_e \theta_e \\ &= [\dot{\hat{\theta}}_u \theta_e - \max[\dot{\hat{\theta}}_u] sign(\theta_e)\theta_e] - K\theta_e^2 \\ &\leq 0 \end{aligned} \tag{30}$$

Therefore, for the cases that the obstacle does not move, the proposed guidance command based on the differential geometry guarantees the obstacle avoidance.

6 SIMULATION RESULTS

Numerical simulation is performed to verify the performance and reliability of the proposed formation reconfiguration algorithm. Initial formation pattern is V-shape, and a leader UAV is the one in vertex. As shown in Fig. 6, formation fleet of 5 UAVs is preserved since DG command for the outermost vehicle does not exceed the limit in Eq.(15). Note that the black point in the center of the figure denotes the guidance transtion moment from the avoidance guidance to the goal tracking one. Figure 8 shows the trajectory of each UAV for the collision avoidance to the obstacle. Note that UAV 2 and UAV 4 are separated from the initial formation fleet. In accordance with the formation reconfiguration process, UAV 2 becomes a new leader of sub-group consisting of UAV 2 and UAV 4. Figures 7 and 9 show the relative distance between UAVs and obstacle for the formation preserving case and separting case, respectively. Safety radius of each vehicle is sustained faithfully.

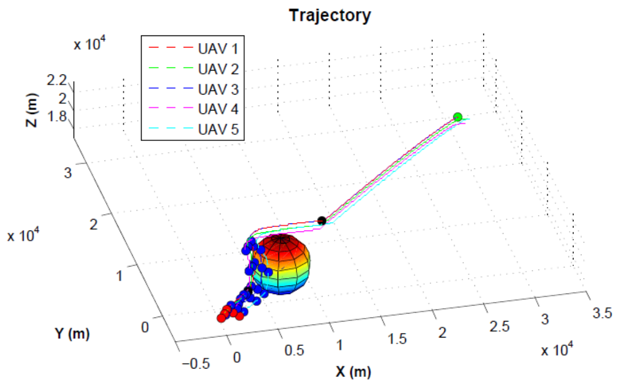

Fig. 6 Trajectory of UAVs with obstacle - formation preserved

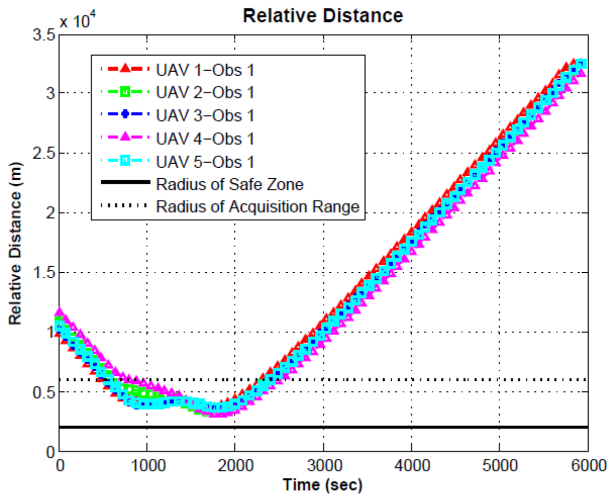

Fig. 7 Relative distance between UAVs and obstacle - formation preserved

7 CONCLUSIONS AND FUTURE WORKS

Formation reconfiguration process is proposed to achieve the formation keeping and collision avoidance simultaneously. Proposed differential geometry based guidance strategy makes it possible for multiple UAVs to avoid colliding with the obstacle while keeping the given formation. The proposed decision making protocol makes the formation flight preserve their geometrical format during the obstacle avoidance without collision between UAVs. For the case that formation cannot be maintained, formation reconfiguration strategy is used to make command split

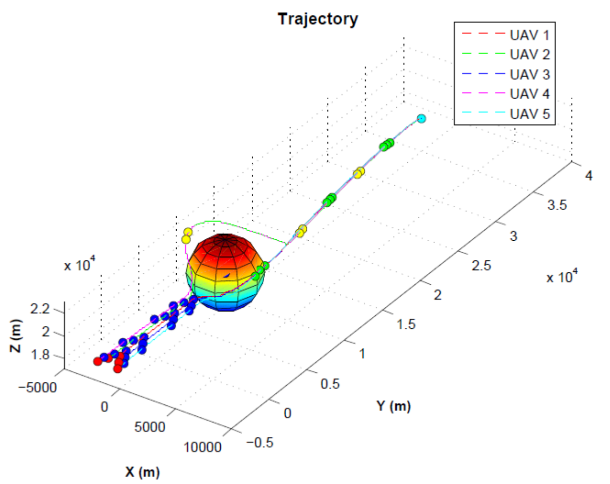

Fig. 8 Trajectory of UAVs with obstacle - formation separated

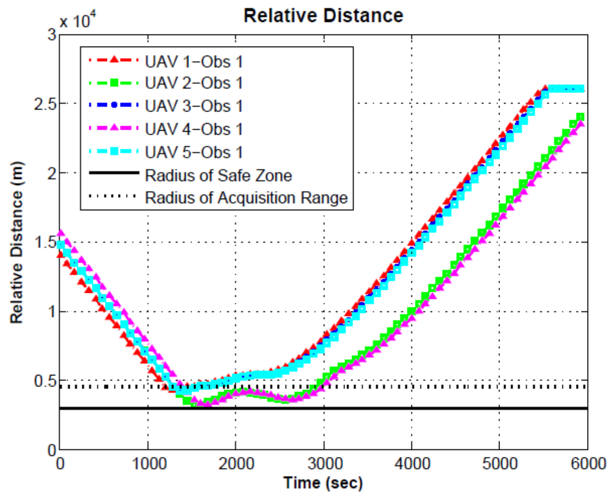

Fig. 9 Relative distance between UAVs and obstacle - formation separated

the current formation up into sub group and distribute a guidance control to each group for collision avoidance. Lyapunov stability theory is used to analyze the stability of the guidance strategy based on differential geometry. Adaptive collision avoidance and 3-dimensional approach will be performed as a further study.

8 ACKNOWLEDGMENTS

This work was supported by Defense Acquisition Program Administration and Agency for Defense Development under the contract UD100048JD.

9 COPYRIGHT STATEMENT

The authors confirm that they, and/or their company or organization, hold copyright on all of the original material included in this paper. The authors also confirm that they have obtained permission, from the copyright holder of any third party material included in this paper, to publish it as part of their paper. The authors confirm that they give permission, or have obtained permission from the copyright holder of this paper, for the publication and distribution of this paper as part of the ICAS2012 proceedings or as individual off-prints from the proceedings.

References

[1] H. S. Shin, A. Tsourdos, B.A. White, M. Shanmugavel, and M. J. Tahk. “UAV Conflict Detection and Resolution for Static and Dynamic Obstacles," *AIAA Guidance, Navigation and Control Conference*, Honolulu, HI, Aug. 2008.

[2] G. Dowek, and C. Munoz, “Conflict Detection and Resolution for 1, 2, .., N Aircraft," *7th AIAA Aviation Technology, Integration and Operations Conference*, Belfast, Northern Ireland, Sep. 2007.

[3] S. J. Kim, I. H. Whang, and C. Song, “Guidance Law for Formation Flight via Desired Position," *IEEE International Symposium on Industrial Electronics*, Seoul, Korea, Oct. 2009.

[4] A. Mujumdar, and R. Padhi, “Reactive Collision Avoidance Using Nonlinear Geometric and Differential Geometric Guidance," *Journal of Guidance, Control, and Dynamics*, Vol. 34, No. 1, 2011, pp 303-310.

[5] B. A. White, R. Zbikowski, and A. Tsourdos, “Direct Intercept Guidance using Differential Geometry Concepts,” *IEEE Transactions on Aerospace and Electronics Systems*, Vol 43, No. 3, 2007, 899-919.

[6] S. Venkataramanan, and A. Dogan, “A Multi-UAV Simulation for Formation Reconfiguration," *AIAA Modeling and Simulation Technologies Conference*, Providence, RI, Aug. 2004.